Journal of Southeast University (English Edition) Vol. 28, No. 4, pp. 428 - 433 Dec. 2012 ISSN 1003—7985

High-precision automatic measurement of two-dimensional geometric features based on machine vision

He Boxia He Yong Xue Rong Yang Hongfeng

(School of Mechanical Engineering, Nanjing University of Science and Technology, Nanjing 210094, China)

Abstract: To realize high-precision automatic measurement of two-dimensional geometric features on parts, a cooperative measurement system based on machine vision is constructed. Its hardware structure, functional composition and working principle are introduced. The mapping relationship between the feature image coordinates and the measuring space coordinates is established. The method of measuring path planning of small field of view (FOV) images is proposed. With the cooperation of the panoramic image of the object to be measured, the small FOV images with high object plane resolution are acquired automatically. Then, the auxiliary measuring characteristics are constructed and the parameters of the features to be measured are automatically extracted. Experimental results show that the absolute value of relative error is less than 0.03% when applying the cooperative measurement system to gauge the hole distance of 100 mm nominal size. When the object plane resolving power of the small FOV images is 16 times that of the large FOV image, the measurement accuracy of small FOV images is improved by 14 times compared with the large FOV image. It is suitable for high-precision automatic measurement of two-dimensional complex geometric features distributed on large scale parts.

Key words: machine vision; two-dimensional geometric features; high-precision measurement; automatic measurement

doi: 10.3969/j.issn.1003-7985.2012.04.010

In some manufacturing industries such as precision machinery and household appliances, the measurement of two-dimensional geometric features, especially complex features such as curves and hole distance, is inefficient and unstable, which has greatly restricted the production levels on the spot of large batch assembly line production. In recent years, with the rapid development of advanced manufacturing technology, the test and metrological technology is required to change from traditional non-spot to manufacturing spot and from traditional afterwards measurement to in-process measurement[1]. It has been an important developing direction to realize high-precision, large range, automatic and digital measurement at the manufacturing spot[2]. Because of the advantages of non-contact, rich information, easy-to-get automatization and intellectualization, machine vision measurement (MVM) has become an innovative approach for measurement and inspection in the manufacturing process[3-4].

In the existing MVM technologies of two-dimensional geometric features, the study and the application of microscopic feature measurement and control with high-precision and automatization are relatively successful[5-6]. This is owing to the fact that the target can be observed with high resolution in a single image while the measuring scope is small[7]. When the feature size is up to 50 to 500 mm or even larger, in order to obtain higher measurement accuracy, the image with a high object plane resolution is required. In this aspect, two MVM methods that are respectively based on image mosaic technology[8] and sequential partial images[9] have made some useful exploration. However, when the amount of high resolution images that need mosaic technology is numerous, the MVM using mosaic technology can hardly meet the demands of fast in-situ measurements. Moreover, this method needs to artificially add the characteristics of the points or lines on the parts to be measured, which is inconvenient to be carried out on the spot of automatic measurement[10]. As for the MVM technology based on sequential partial images, it only applies to the measurement of straight edge parts and linear geometric features[11]. Furthermore, it does not have the function of automatic measurement. In industrial practice, the measurement system integrating MVM technology with CMM has achieved good effects[12]. However, this scheme still cannot realize automatic measurement due to the lack of the whole information of the parts to be measured. In addition, its measurement accuracy depends on the precision of mechanical coordinates. The high-precision mechanical coordinates will bring about a complex measurement system, high manufacturing cost, high requirements for the control over the measurement environments such as temperature and the subsequent high use cost.

To realize high-precision automatic measurement of the two-dimensional complex geometric features on larger parts, an MVM system with the cooperation of multiple FOV is constructed.

Received 2012-07-21.

Biographies: He Boxia (1972—), male, doctor, lecturer, heboxia@163.com; He Yong (1964—), male, doctor, professor, yhe1964@mail.njust.edu.cn.

Foundation items: The National Natural Science Foundation of China (No. 51175267), the Natural Science Foundation of Jiangsu Province (No. BK2010481), the Ph.D. Programs Foundation of Ministry of Education of China (No. 20113219120004), China Postdoctoral Science Foundation (No. 20100481148), the Postdoctoral Science Foundation of Jiangsu Province (No. 1001004B).

Citation: He Boxia, He Yong, Xue Rong, et al. High-precision automatic measurement of two-dimensional geometric features based on machine vision[J]. Journal of Southeast University (English Edition), 2012, 28(4): 428 - 433. [doi: 10.3969/j.issn.1003-7985.2012.04.010]

1 Cooperative Measurement System Based on Machine Vision

1.1 Hardware and functional composition

The cooperative measurement system based on machine vision is constructed as shown in Fig. 1. It is mainly composed of the mechanical subsystem, the optical imaging subsystem, the motion control subsystem, the image acquisition subsystem, the image processing subsystem and the database subsystem. The mechanical subsystem is used to construct the physical space for automatic measurement. It consists of *XYZ* three-directional moving coordinates and the rotating mechanism of a small FOV camera. The optical imaging subsystem is composed of a light source, a large FOV lens and a small FOV telecentric lens. The motion control subsystem controls the displacement of the three coordinates and the rotation of the small FOV camera. The image acquisition subsystem automatically collects the panoramic image of large FOV and sequential images of small FOV. The image processing subsystem mainly completes the tasks of identifying the features to be measured in the large FOV image, planning the measuring path of small FOV images and extracting the dimensional characteristics in sequential small FOV images. The database subsystem stores the direction and position data of the features identified in the large FOV image. The parameters of the measured features are also stored in the database.

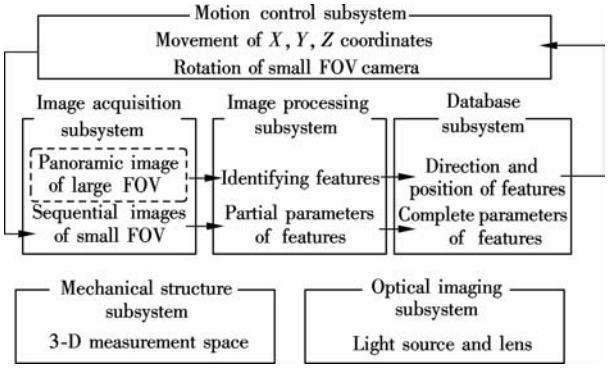

Fig. 1 Composition of the cooperative measurement system

1.2 Working principle

The working principle and steps of the cooperative measurement system are as follows:

1) Calibrating measuring space and identifying features to be measured

A three-dimensional measuring space $O_M XYZ$ is constructed as shown in Fig. 2. Suppose that the area of the objects to be measured is F_0. First, the measuring plane is calibrated at O_1 and the panoramic image of the target area S_{11} is taken at O_1. It should be ensured that the imaging FOV F_{11} is a little bigger than F_0. Then, the mapping relationship between the image coordinate and the measuring space coordinate is established. After that, the features to be measured are identified in the large FOV image and the direction and position coordinates of these features in the measuring space are calculated.

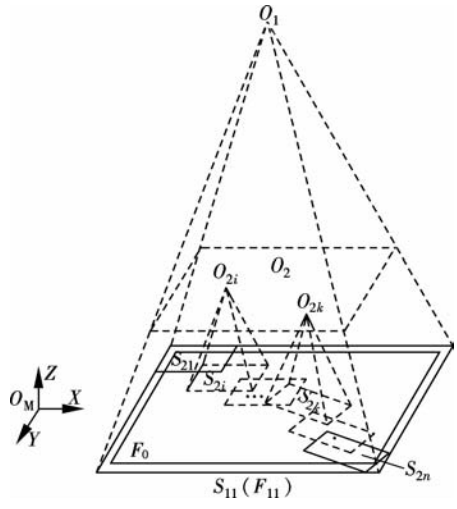

Fig. 2 Illustration of the measuring space

2) Planning measuring path of small FOV images and acquiring small FOV images

According to the size of the small FOV and the direction and position of the features to be measured, an optimized acquisition path of the small FOV images is obtained through the specific algorithm. Then, the sequential small FOV images are automatically collected according to the path. As shown in Fig. 2, O_2 is the plane of the camera position while acquiring the sequential small FOV images $S_{2i}(i = 1, 2, \ldots, n)$. It should be noted that the image plane $S_{2k}(1 \leqslant k \leqslant n)$ is rotated relative to the large FOV image S_{11}

3) Extracting parameters of features to be measured

According to the position of the small FOV images in the measuring space and the distribution of the geometrical features in the images, the auxiliary measuring characteristics are constructed in the overlapping areas of the sequential small FOV images and the homonymous characteristics are matched. After that, in each small FOV image, the partial parameters of the features to be measured are extracted through the coordinates of the features and the auxiliary measuring characteristics. Then the local measuring errors are estimated and compensated for. Finally, in accordance with the direction and position of the small FOV sequential images in the measuring space, the local parameters are added up and the whole parameters of the features to be measured are derived.

2 Relationship Between Image Coordinates and Measuring Space Coordinates

As shown in Fig. 3, a measuring space coordinate system $O_M XYZ$ is established, which is the physical space where all the measuring activities are carried out. Suppose that the target to be measured is located in the plane $XO_M Y$. $O_M XY$ is addressed as a measuring plane coordinate system. The camera optic axis oo' is always parallel to axis *Z*. The fields of view with different sizes can be obtained through adjusting the *Z* coordinate value of the point

o' in $O_M XYZ$. Different regions of the measuring plane can be imaged by altering the X coordinate value and/or the Y coordinate value of the point o'. oxy is the object plane coordinate system, which is used to determine the direction and position of the imaging FOV in the measuring space. oxy and $O_M XY$ are in the same plane. The origin o is the intersection of the camera optical axis and the measuring plane. o_1uv is the image coordinate system. The axis u represents the horizontal ordinate of the image, which is parallel to the x axis of the object plane coordinates. The v axis is the vertical coordinate of the image, which is parallel to the y axis. The unit of the image coordinates can be pixels or floating-point numbers[11].

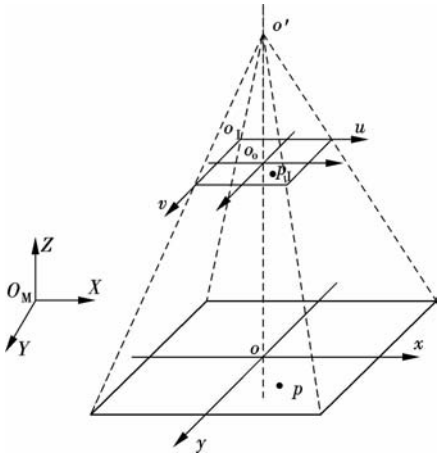

Fig. 3 Measuring space coordinate system, object plane coordinate system and image coordinate system

Suppose that p is a point in a two-dimensional target. Its coordinate in oxy is (x, y) and in $O_M XY$ is (X, Y). The relationship between the object plane coordinates and the measuring plane coordinates can be expressed as

$$\begin{bmatrix} X \\ Y \\ 1 \end{bmatrix} = \begin{bmatrix} \cos\theta & -\sin\theta & X_o \\ \sin\theta & \cos\theta & Y_o \\ 0 & 0 & 1 \end{bmatrix} \begin{bmatrix} x \\ y \\ 1 \end{bmatrix} = \begin{bmatrix} \boldsymbol{R} & \boldsymbol{T} \\ \boldsymbol{0}^{\mathrm{T}} & 1 \end{bmatrix} \begin{bmatrix} x \\ y \\ 1 \end{bmatrix} = \boldsymbol{C} \begin{bmatrix} x \\ y \\ 1 \end{bmatrix} \tag{1}$$

where θ is the rotating angle of the object plane over the measuring plane; $\boldsymbol{R}$ is the rotating matrix; $\boldsymbol{T}$ is the two-dimensional translation vector with $\boldsymbol{T} = [X_o \ Y_o]^{\mathrm{T}}$, which is the coordinate vector of o in $O_M XY$; and $\boldsymbol{C}$ is the coordinate transformation matrix.

After the measurement system is calibrated, suppose that the pixel equivalent of the object plane coordinate scale in the image coordinate system is δx and δy and the projection of point $p(x, y)$ in the image coordinate system is $p_1(u, v)$. The relationship between the image coordinates and the object plane coordinates can be derived as

$$\begin{bmatrix} x \\ y \\ 1 \end{bmatrix} = \begin{bmatrix} \delta_x & 0 & -u_o\delta_x \\ 0 & \delta_y & -v_o\delta_y \\ 0 & 0 & 1 \end{bmatrix} \begin{bmatrix} u \\ v \\ 1 \end{bmatrix} = \boldsymbol{Q} \begin{bmatrix} u \\ v \\ 1 \end{bmatrix} \tag{2}$$

where (u_o, v_o) is the image coordinate of o_o, which is the projection of o, i. e., the center point of the image.

Substituting $[x, y, 1]^{\mathrm{T}}$ into Eq. (1), the mapping relationship between the image coordinates and the measuring plane coordinates is obtained as

$$\begin{bmatrix} X \\ Y \\ 1 \end{bmatrix} = \begin{bmatrix} \boldsymbol{R} & \boldsymbol{T} \\ \boldsymbol{0}^{\mathrm{T}} & 1 \end{bmatrix} \begin{bmatrix} \delta_x & 0 & -u_o\delta_x \\ 0 & \delta_y & -v_o\delta_y \\ 0 & 0 & 1 \end{bmatrix} \begin{bmatrix} u \\ v \\ 1 \end{bmatrix} = \boldsymbol{CQ} \begin{bmatrix} u \\ v \\ 1 \end{bmatrix} \tag{3}$$

where $\boldsymbol{CQ}$ is a 3×3 invertible matrix. Thus, the following equation can also be derived as

$$[u \quad v \quad 1]^{\mathrm{T}} = \boldsymbol{Q}^{-1}\boldsymbol{C}^{-1}[X \quad Y \quad 1]^{\mathrm{T}} \tag{4}$$

where

$$\boldsymbol{Q}^{-1} = \begin{bmatrix} 1/\delta_x & 0 & u_o \\ 0 & 1/\delta_y & v_o \\ 0 & 0 & 1 \end{bmatrix}$$

$$\boldsymbol{C}^{-1} = \begin{bmatrix} \cos\theta & \sin\theta & -X_o\cos\theta - Y_o\sin\theta \\ -\sin\theta & \cos\theta & X_o\sin\theta - Y_o\cos\theta \\ 0 & 0 & 1 \end{bmatrix}$$

It is clear that the mapping relationship between the image coordinates and the measuring space coordinates is established by Eqs. (3) and (4). The specific values can be figured out as long as $\boldsymbol{R}$, $\boldsymbol{T}$, δx and δy are known.

3 Measuring Path Planning of Small FOV Images

After the features to be measured are identified in the large FOV image, the measuring path of small FOV images can be planned according to the size of the small FOV and the shape, the direction and the position of the features in the large FOV image. Two problems must be solved when the measuring path is planned. One is how to determine the numbers of the small FOV images; the other is how to obtain the measuring space coordinates of every image. The measuring path must satisfy four basic conditions: 1) The features to be measured or partial characteristics in small FOV images should be easy to be identified and the identification accuracy should be as high as possible; 2) In a segment of the measuring path, the angle of the image plane should be kept consistent to avoid the difficulties of feature matching caused by the relative rotation between images; 3) The auxiliary measuring characteristics should be parallel to the row or column direction of the image, which can ensure the accuracy of matching the homonymous characteristics; 4) Under the condition that the auxiliary measuring characteristics can be matched reliably, the number of small FOV images should be minimal to minimize cumulative errors. For the specific features to be measured, which are constrained by the above four conditions, an optimized measuring path can be figured out.

As shown in Fig. 4, the measurement of the hole distance between O_1 and O_2 is taken as an example to explain

the method of the measuring path planning of small FOV images. According to the conditions 2) and 3), the acquisition of the small FOV sequential images should be along the center line O_1O_2. According to the condition 1), the round hole should be imaged near the image center as shown in Fig. 4 (a). This can eliminate the influence of distortions and obtain higher accuracy of the feature hole. According to the condition 4), in order to minimize the numbers of small FOV images, the two round holes should be imaged near the image edge as shown in Fig. 4 (b). Thus, there are two schemes for choice as indicated in Fig. 4(a) and Fig. 4(b). The test shows that the measuring accuracy of the hole distance mainly depends on the coordinate accuracy of the hole centers and the matching accuracy of the sequential images. Therefore, the scheme shown in Fig. 4(a) is more conducive to improving the measurement accuracy. In this scheme, the center of the first small FOV image is coincident with the center of the first hole. The coordinates of its collecting position in the measuring space can be obtained by substituting the image coordinate of the hole center in the large FOV image into Eq. (3). The acquisition parameters of the remaining small FOV images can be calculated by the following equations:

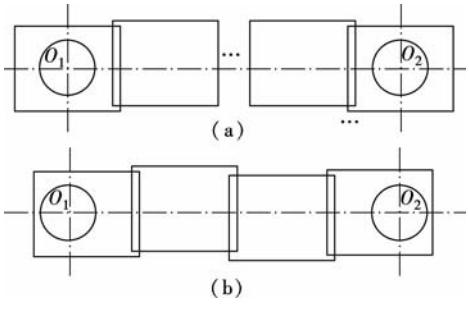

Fig. 4 Illustration of measuring path planning. (a) Round hole near the image center; (b) Round hole near the image edge

$$n = n_1 + 2 \tag{5}$$

$$n_1 = \text{ceil}\left(\frac{D-H}{H-e\delta}\right) \tag{6}$$

$$m_1 = \frac{1}{2}\left(H + \frac{D-H}{n_1}\right) \tag{7}$$

$$m_2 = \frac{D-H}{n_1} \tag{8}$$

where n is the total number of small FOV images that need to be collected between two holes; n_1 is the number of small FOV images except the first and the n-th image; m_1 is the moving distance from the position of collecting the first image to that of collecting the second image. The displacement of the n-th image relative to the $(n-1)$-th image is also m_1. m_2 is the displacement of collecting the k-th($k = 3, 4, \ldots, n-1$) image relative to the $(k-1)$-th image; D represents the distance between two holes, which can be substituted with the measured value in the large FOV image; H represents the transverse size of the small FOV; δ is the pixel equivalent value of small FOV images; e is the displacement error factor of the measuring device, and it generally takes the value of three times the locating error; ceil(·) is the rounding function, i.e., to take the smallest integer greater than or equal to the value of the expression.

4 Experiment and Results

The part to be measured is an instrument base. The diameter of the circular base is ϕ150 mm. Six round holes O_1 to O_6 with ϕ10 mm nominal diameter are evenly distributed along the circumference of ϕ100 mm in the base. They are used to locate six spindles. The positions of the six holes need to be precisely controlled. Their relative locations can be referred to in Fig. 5. The application of the cooperative measurement system is illustrated through the experiment of measuring the distances of O_1O_4, O_2O_5, and O_3O_6.

In the experiment, two Basler CCD cameras with resolutions of 1 390 × 1 038 pixels and 2 448 × 2 050 pixels are adopted, which are labeled as No. 1 and No. 2, respectively. The No. 1 camera is used to collect the large FOV image in the measuring space while the No. 2 to collect the sequential images of small FOV. The No. 1 camera is matched with a fixed focal lens. The FOV is 208.08 mm × 155.39 mm when imaging clearly. In these settings, it can take a full image of the object to be measured. The No. 2 camera is allocated with a telecentric lens. The FOV is set to be 22.89 mm × 19.17 mm. It is used to observe the holes with high accuracy. The measurement system is calibrated with a national second class standard line scale. The calibrating data of the system are given in Tab. 1.

Tab. 1 Calibration data

Camera	δ/(mm · pixel^{-1})
No. 1	0.149 7
No. 2	0.009 35

After calibrating the system, the large FOV image of the part to be measured is collected by the No. 1 camera, which is shown in Fig. 5. In this experiment, the imaging parameters of the large FOV are as follows:

$$\boldsymbol{R}_0 = \begin{bmatrix} 1 & 0 \\ 0 & 1 \end{bmatrix},\ \boldsymbol{T}_0 = \begin{bmatrix} 152.0 \\ 91.3 \end{bmatrix},\ \begin{bmatrix} u_o \\ v_o \end{bmatrix} = \begin{bmatrix} 695.5 \\ 519.5 \end{bmatrix}$$

$$\delta_x = \delta_y = \delta_1 = 0.149\,7$$

According to Eq. (3), the point (X, Y) in the measuring plane corresponding to the pixel point (u, v) in the large FOV image is obtained by

$$\begin{bmatrix} X \\ Y \\ 1 \end{bmatrix} = \begin{bmatrix} 0.149\,7 & 0 & 47.883\,7 \\ 0 & 0.149\,7 & 13.530\,9 \\ 0 & 0 & 1 \end{bmatrix} \begin{bmatrix} u \\ v \\ 1 \end{bmatrix} \tag{9}$$

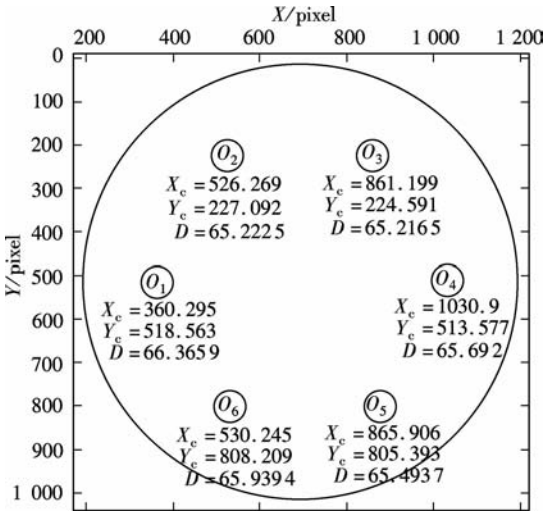

Fig. 5 Features and pixel coordinates identified in large FOV image

After identifying the features in the large FOV image, the pixel coordinates of the center of circular holes (X_c, Y_c) and their diameters can be obtained through fitting the boundary points of the identified features. The results are shown in Fig. 5. The values of the holes distances and the measuring space coordinates of O_1 to O_6 are calculated according to Eq. (9), which are listed in Tab. 2.

Tab. 2 Coordinates and size of the features in large FOV

Number of holes	(X_c, Y_c)/mm	Φ_i/mm	$D_{i,i+3}$/mm	θ_i/(°)
O_1	(101.819 8, 91.159 7)	9.935	100.392	180
O_4	(202.209 4, 90.413 3)	9.834		
O_2	(126.666 1, 47.526 5)	9.764	100.398	120
O_5	(177.509 8, 134.098 2)	9.804		
O_3	(176.805 1, 47.152 1)	9.763	100.437	60
O_6	(127.261 3, 134.519 7)	9.871		

By substituting the distance $D_{i,i+3}$ listed in Tab. 2 into Eqs. (6) to (8), the acquired direction and position of the small FOV sequential images are obtained. The measuring path is shown in Fig. 6

After collecting the small FOV images, the auxiliary measuring characteristics are constructed and matched. As shown in Fig. 7, dimensional characteristics f_{ij} ($i = 1, 2, \cdots, 3; j = 1, 2, \cdots, 6$) are constructed in sequential images S_{ij}. In order to simplify the calculation of the search area for the matched characteristic f'_{ij}, f_{ij}, the characteristic to be matched should be located in the central sections of the overlapping areas. The matched characteristic f'_{ij} is searched in the sequential image $S_{1,i+3}$. After eliminating the gross errors of the matched points, the mean value of the abscissa of the matched points is taken, and the numerical coordinate $\mathrm{dcx}(f'_{ij})$ of f'_{ij} is derived.

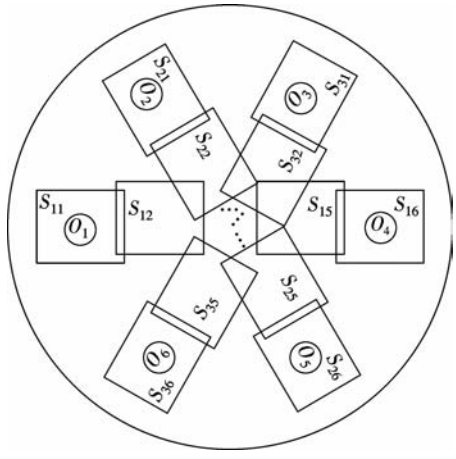

Fig. 6 Illustration of the measuring path of small FOV images

In Fig. 7, G_{i1} is the distance between the center of O_i and the auxiliary measuring characteristic f_{i1}. The coordinates of the circle centre are derived by fitting the pixel points located in the circumference of the holes. G_{i2} is the distance between the center of O_{i+3} and the auxiliary measuring characteristic f'_{i5}. L_{ij} is the distance between the dimensional characteristic line $f_{i,j+1}$ and the matched line f'_{ij}. $D_{i,i+3}$ is the hole distance between O_i and O_{i+3}. These dimensional characteristics can be calculated using the measuring method based on sequential partial images[11].

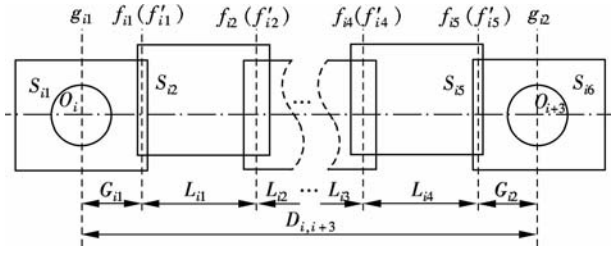

Fig. 7 Schematic diagram of measurement of small FOV images

The measured values of the distances between six holes are given in Tab. 3. From Tab. 3, it can be seen that the absolute value of relative errors is less than 0.03% when using small FOV images to gauge the holes distances. The measurement accuracy of the small FOV images is improved by more than 12 times compared with that of the large FOV image. This proves that it is reasonable to use the large FOV image to guide and small FOV images to measure in the cooperative measurement system.

Tab. 3 Results of the cooperative measurement

Holes distances	Value of dimension characteristics/pixel						Measured value L_i/mm	CMM measured value/mm	Relative error/%
	G_{i1}	L_{i1}	L_{i2}	L_{i3}	L_{i4}	G_{i2}			
O_1O_4	1 117.08	2 159.07	2 060.48	2 060.24	2 159.99	1 143.76	100.051	100.069	−0.018
O_2O_5	1 133.78	2 157.36	2 058.20	2 061.18	2 155.09	1 136.31	100.063	100.088	−0.025
O_3O_6	1 131.40	2 157.65	2 059.27	2 058.97	2 157.79	1 144.97	100.139	100.111	+0.028

5 Conclusion

Aiming at the requirements of high-precision, large range, automatic and digital measuring and detecting technology on the advanced manufacturing spot, a cooperative measurement system based on machine vision is set up. Its composition and principle are introduced. The mapping relationship between the image coordinates and the measuring space coordinates is established. The method of planning the measuring path is developed. Experimental results verify that the cooperative measuring method can realize the high-precision automatic measurement of two-dimensional geometric features on large size parts. The cooperative measurement system well regulates the commonly existing contradiction between the resolution and the measuring range in the MVM. Meanwhile, it fully exploits the potentials of physical features of the imaging device. It has the advantages of simple structure, low use cost and high digital degree. Its measuring accuracy is not affected by the precision of the mechanical coordinates. It is suitable for high-precision automatic measurement of two-dimensional geometric features in the field of industry.

References

[1] Ye Shenghua, Qin Shuren. Development of modern measuring metrological and instrumental technologies [J]. *China Measurement & Test*, 2009, **35**(2):1 - 6. (in Chinese)

[2] Department of Engineering and Materials Sciences, National Natural Science Foundation of China. *Report of the development strategy of mechanical engineering science* (2011—2012) [M]. Beijing: Science Press, 2010. (in Chinese)

[3] Weckenmann A, Jiang X, Sommer K D, et al. Multisensor data fusion in dimensional metrology [J]. *CIRP Annals-Manufacturing Technology*, 2009, **58**(2): 701 - 721.

[4] Mar N S S, Yarlagadda P K D V, Fookes C. Design and development of automatic visual inspection system for PCB manufacturing [J]. *Robotics and Computer-Integrated Manufacturing*, 2011, **27**(5): 949 - 962.

[5] Yoon H S, Chung S C. Vision inspection of micro-drilling processes on the machine tool [J]. *Transactions of the North American Manufacturing Research Institute of SME*, 2004, **32**:391 - 398.

[6] Dutta S, Datta A, Chakladar N D, et al. Detection of tool condition from the turned surface images using an accurate grey level co-occurrence technique [J]. *Precision Engineering*, 2012, **36**(3): 458 - 466.

[7] Sun T H, Tseng C C, Chen M S, et al. Electric contacts inspection using machine vision [J]. *Image and Vision Computing*, 2010, **28**(6): 890 - 901.

[8] Quan Yanming, Li Shumei. Fast image mosaic method for large-scale workpiece measurement system [J]. *Journal of South China University of Technology: Natural Science Edition*, 2011, **39**(8):60 - 65. (in Chinese)

[9] He Boxia, Zhang Zhisheng, Dai Min, et al. A novel method of machine vision measurement based on sequential partial images [C]//*Proceedings of the International Conference on Mechanical Engineering and Mechanics*. Wuxi, China, 2007:561 - 566.

[10] Niu Xiaobing, Lin Yuchi, Zhao Meirong, et al. Study on 2-D image connection and its application in geometrical parameters measurement [J]. *Journal of Tianjin University: Science and Technology*, 2001, **34**(3): 396 - 399. (in Chinese)

[11] He Boxia, Zhang Zhisheng, Dai Min, et al. A high-precision dimension measurement method based on sequential partial images [J]. *Optics and Precision Engineering*, 2008, **16**(2): 367 - 373. (in Chinese)

[12] Subramanian R, de St Germain H J, Drake S. Integrating a vision system with a coordinate measuring machine to automate the datum alignment process [C]//*Proceedings of the ASME International Design Engineering Technical Conferences and Computers and Information in Engineering Conference*. Long Beach, CA, USA, 2005: 655 - 661.

二维几何特征的机器视觉高精度自动测量

何博侠　何　勇　薛　蓉　杨洪锋

(南京理工大学机械工程学院, 南京 210094)

摘要:为了对零件上二维几何特征进行高精度自动测量,建立了机器视觉协同测量系统. 介绍了系统的硬件组成、功能结构及工作原理,建立了特征图像坐标与测量空间坐标之间的映射关系,提出了小视场图像测量路径的规划方法. 在被测目标全景图像信息的协同下,自动采集具有高物面分辨率的小视场序列图像,自动构造辅助测量特征并提取被测特征的参数. 应用该系统测量 100 mm 的孔距,结果表明:相对误差的绝对值不超过 0.03%;当小视场图像的物面分辨力是大视场图像的 16 倍时,小视场图像的测量精度比大视场图像平均提高 14 倍. 故该系统适用于对大尺寸零件上分布的二维复杂几何特征进行高精度自动测量.

关键词:机器视觉;二维几何特征;高精度测量;自动测量

中图分类号:TP216;TH741